

Observing Dark Matter in the Galactic Spectrum?

by

Kyle Lawson

B.Sc., The University of Western Ontario, 2005

A THESIS SUBMITTED IN PARTIAL FULFILLMENT OF
THE REQUIREMENTS FOR THE DEGREE OF

MASTER OF SCIENCE

in

The Faculty of Graduate Studies

(Physics)

THE UNIVERSITY OF BRITISH COLUMBIA

(Vancouver)

October, 2008

© Kyle Lawson 2008

Abstract

Observations from a broad range of astrophysical scales have forced us to the realization that the well understood matter comprising the stars and galaxies we see around us accounts for only a small fraction of the total mass of the Universe. An amount roughly five times larger exist in the form of dark matter about which we have virtually no direct evidence apart from its large scale gravitational effects. It is also known that the largest contribution to the energy density of the universe is the dark energy, a negative pressure form of energy which will not be dealt with here.

I will present a candidate for the dark matter which is based completely in known physics and which presents several possible observational signatures. In this model the dark matter is composed of dense nuggets of baryonic matter and antimatter in a colour superconducting state. If these object are sufficiently massive their low number density will make them effectively dark in the sense that collisions with visible matter become infrequent. This work presents the basics of dark matter as a colour superconductor and then uses the physical properties of the quark nuggets to extract observational consequences.

Table of Contents

Abstract	ii
Table of Contents	iii
List of Figures	v
1 Introduction	1
1.1 Dark matter	1
1.2 Bayogenesis	1
1.3 Motivation	2
2 Nugget structure	4
2.1 Colour superconductivity	4
2.2 The electrosphere	5
3 Emission mechanisms	7
3.1 Electron annihilation	7
3.2 Comparison with observation	9
3.2.1 The galactic 511keV line	9
3.2.2 Diffuse MeV emissions from the galactic core	9
3.2.3 Other emission mechanisms	10
4 Conclusion	15
Bibliography	16
Appendices	
A Lepton Distributions	18
B Positronium Formation Rates	21

Table of Contents

C The direct annihilation spectrum 23

List of Figures

3.1	Best fit to the high energy diffuse spectrum of the galactic centre from Moskalenko et al. based on cosmic ray effects with point sources subtracted. Note the observed excess over the calculated spectrum in the COMPTEL range.	13
3.2	Total intensity (flattened by k^2 as in 3.2.2) averaged over all electrosphere heights. The total emission spectrum is shown in solid blue while the cosmic ray background and dark matter spectrum are shown in black dotted and dashed lines respectively. The red bars are the COMPTEL data points.	14
A.1	Chemical potential as a function of height. Here the surface chemical potential is taken to be $\mu_0 = 30MeV$	19
A.2	Lepton density as a function of height. Here the surface chemical potential is taken to be $\mu_0 = 30MeV$	20
C.1	Spectral density as a function of photon energy (with arbitrary normalization.) Plotted for $\mu = 10MeV$ (blue), $\mu = 30MeV$ (green) and $\mu = 60MeV$ (red.) The spectra have been rescaled by $\frac{1}{\mu}$ for to allow multiple curves on the same axes.	24

Chapter 1

Introduction

1.1 Dark matter

A growing list of observations have demonstrated that the majority of the mass in the galaxy is in the form of dark matter (DM.) At the same time we are without an established physical theory to explain it's fundamental nature. Consistency with observation requires that DM must interact very minimally with the ordinary matter comprising the visible universe. However, it's gravitational influence is critical in shaping the cosmological structures seen today. Any candidate must produce no observational signature and be stable on cosmological time scales. While no definitive DM candidate is known the majority of models work within the context of the weakly interacting massive particle (WIMP) paradigm. WIMP models of dark matter generally introduce a new fundamental field which couples only weakly to visible matter. As there are no known particles with suitable properties any such model must invoke new physics. If the mass and coupling strength of the field comprising the dark matter are known then the present day abundance (which is the only definitively observed parameter) may be calculated.

An interesting aspect of dark matter is that its energy density in the present universe is of comparable scale to that of the visible matter component with, $\Omega_{DM} \sim 5\Omega_{vis}$. If the energy scales at which dark matter forms are dramatically different from the QCD scale which determines the matter component of the energy density then fine tuning of the parameters of the dark sector becomes necessary to explain the similar energy densities.

1.2 Baryogenesis

A second puzzle of modern cosmology which will be addressed here is the nature of baryogenesis. Observations show that the Universe is composed almost entirely of matter as opposed to antimatter yet physical laws seem to treat the two identically making this dichotomy difficult to explain. The

necessary conditions to explain the prevalence of matter are known as the Sakharov conditions, any plausible explanation must contain mechanisms to produce Baryon number violations, CP violations and must involve non-equilibrium physics. In practice this generally involves driving a CP violating process at a phase transition when the universe is far from equilibrium. As with the case of dark matter there have been many models put forward to explain baryogenesis however they all require physics beyond the standard model and in many cases involve some fine tuning of the parameters of this new physics.

1.3 Motivation

These two, seemingly unrelated, problems of modern cosmology may be addressed through a single theory if the one assumes that both baryogenesis and dark matter formation occur at the QCD phase transition in the early universe. It has been suggested that there may be mechanisms operating at the phase transition which are capable of compacting matter to extremely large baryon density and that these processes operate in a manner in which CP violation happens with a probability of order one. Some evidence for the charge separation mechanism necessary for this process may in fact be seen in recent QGP experiments at RHIC in Brookhaven [6].

In what follows I will accept that these mechanisms do operate at the QCD phase transition and that they are capable of compressing the condensing baryonic matter to the point where it forms nuggets of a dense colour superconducting state the properties of which will be discussed in a subsequent section. In this model there is no baryon number violation involved in the process of baryogenesis. The CP violation makes the process of forming anti-nuggets more efficient than forming nuggets of normal quarks. The remaining matter and antimatter annihilate each other leaving only the heavy quark nuggets and the fraction of excess matter corresponding to the surplus of antimatter nuggets. Calculating the exact rates of formation is not currently feasible but to match present observations requires that the end result of this process is a universe with a mass distribution of roughly $\Omega_{visible} : \Omega_{DM} : \Omega_{\bar{DM}} = 1 : 2 : 3$ where DM and \bar{DM} are dark matter in quark and antiquark nugget form. This ratio would give the correct visible to dark matter ratio and gives a universe with no net baryonic charge. This model is discussed in greater detail in the original papers [14] and [10]. An intensive discussion of the nugget formation mechanisms is beyond the scope of this work. Instead the approach taken here will be to consider the

1.3. Motivation

possible observational consequences of this model and test its consistency with present data and to consider possible future constraints.

Chapter 2

Nugget structure

2.1 Colour superconductivity

At the relatively low atomic scale densities which are experimentally accessible the ground state of baryonic matter is known to be the iron nucleus which minimizes the binding energy per nucleon. However, new lowest energy states are allowed as the density is increases. If the baryon density is taken to be asymptotically large the lowest energy state of QCD is known to be one in which the constituent quarks condense to form Cooper pairs. This state is referred to as colour superconductivity and proceeds through the BCS mechanism familiar from well studied superconductivity in low temperature metals. A wide variety of colour superconductors (CS) are known to be possible depending on the pairing mechanism involved in forming the quark Cooper pairs. It is beyond the scope of the present work to discuss the full range of possible states. A review is available in, for example, [2]. Instead I will focus on the generic features of known CS phases in an attempt to extract general properties of the proposed dark matter candidate. Much of the physics discussed here depends not on the state of the quark matter but simply on the net surface charge. The existence of a net charge is relatively simple to understand though the exact details rapidly become complicated. At asymptotically large densities the quark chemical potential becomes greater than the strange quark mass, $m_s \sim 150 MeV$ and it is energetically favorable for the CS to contain equal numbers of up, down and strange quarks with each flavor allowing a new pairing channel and thus lowering the total energy. In a phase with equal numbers of the three light quark flavors the quark matter is electrically neutral and the presence of leptons is strongly disfavored energetically. However, near the surface of the quark matter the chemical potential drops and with it the fraction of much heavier strange quarks. In this case the quark matter develops a net positive charge in the case of a matter nugget or a net negative charge in the case of a nugget composed of antiquarks. An exact calculation of the surface charge is a complex calculation and dependent on the exact superconducting phase realized, however, it is quite generically found that the lepton chemical

potential at the quark matter surface should lie in the range from 10MeV up to 100MeV while the quark chemical potential is roughly an order of magnitude larger. The binding energy of the surface quarks is at the QCD scale and thus the quark surface is quite sharp, generally on the order of fm. By contrast the leptons are bound only through electromagnetic effects and the looser binding means that they will extend well beyond the quark surface. The distribution of these surrounding leptons will be the subject of the following section.

2.2 The electrosphere

Regardless of the phase of superconductivity realized in the quark matter the nugget will carry a net charge (positive in the case of a matter nugget and negative in the case of an antinugget.) To compensate for the net charge of the quark matter the nuggets will build up a layer of leptons, known as the electrosphere, at its surface. The form of this extended electrosphere has previously been studied in the case of quark stars (see for example [1], [12]). While the quark matter has a very sharp surface at a typical strong force scale the electrosphere will be an extended object with the leptons bound only by the relatively weak electric force. At the mean field level we can model the electrosphere as a fermi gas of leptons. The density distribution of electrons may be determined by equating the degeneracy pressure of the Fermi gas with the electrical attraction due to the charge of the quark matter. This gives a differential equation of the form

$$\nabla^2 \mu = 4\pi\alpha n_l = \frac{4\alpha}{\pi} \int_0^\infty \frac{p^2 dp}{1 + e^{(E-\mu)/T}} \quad (2.1)$$

Where μ is the lepton chemical potential and n_l is the lepton density which is taken to be that of a fermi gas. In the case where the temperature is much less than the chemical potential the momentum integration may be approximated to give,

$$\nabla^2 \mu = \frac{4\alpha}{3\pi} (\mu^2 - m^2)^{3/2} \quad (2.2)$$

Combining this equation with the surface chemical potential $\mu_0 \sim 10 - 100\text{MeV}$ and the requirement that the chemical potential (and electric field) vanishes at spacial infinity allows us to solve for the density at any distance above the quark surface. The general solution to the density equation does not have a simple analytic expression however there are two important

2.2. The electrosphere

regimes in which the solution may be approximated with a simple expression. For reference several numerical solutions are demonstrated in appendix A. The first case is the ultrarelativistic limit which occurs close to the quark surface. In this regime the temperature of the electrosphere and the lepton mass are negligible when compared to the chemical potential. In this case the the density equation takes the form,

$$\frac{d^2\mu}{dz^2} = \frac{4\alpha}{3\pi}\mu^3 \quad (2.3)$$

The solution to this second order differential equation which vanishes as $z \rightarrow \infty$ is,

$$\mu_{e^+}(z) = \sqrt{\frac{3\pi}{2\alpha}} \frac{1}{(z + z_0)}, \quad z_0 = \sqrt{\frac{3\pi}{2\alpha}} \frac{1}{\mu_0}, \quad n_{e^+}(z) \simeq \frac{\mu_{e^+}^3(z)}{3\pi^2} \quad (2.4)$$

The other regime in which the solution has a simple form is in what will be referred to as the Boltzmann regime. The Boltzmann regime should begin at a density of roughly $n = \left(\frac{mT}{2\pi}\right)$ such that there is less than one particle per unit of phase space and degeneracy effects become weak. In this regime the electron mass becomes the largest physically relevant scale. If the Boltzmann regime lies close enough to the quark matter surface that the plane parallel approximation holds an analytic solution to equation 2.1 may be found. In this case the density takes the simplified form,

$$n(z, T) = \frac{T}{2\pi\alpha} \frac{1}{(z + \bar{z})^2} \quad (2.5)$$

While the chemical potential falls exponentially. Here \bar{z} is a constant to be matched to a boundary condition at the start of the Boltzmann regime. The critical fact is that whether it is obtained numerically or for a region in which an approximate solution is known it is possible to express the lepton density and the fermi momentum as a function of radial distance from the quark matter surface. This distribution is essentially independent of the details of the colour superconducting core and may be determined completely from the central charge.

Chapter 3

Emission mechanisms

Conventional dark matter candidates such as WIMPs are generally made dark by their small interaction cross section with visible matter. Observational consequences of a given model may be determined from the form of these interactions. In this case it is entirely possible that there may be no observational signature of the dark matter beyond its gravitational influence. Currently favoured models tend to give the dark matter particles masses at the TeV scale and thus interaction cross sections at the weak scale. Conversely, if the dark matter is composed of quark nuggets as outlined above interactions are suppressed by purely geometric factors. In regions of the galaxy where both the matter and dark matter densities are large one would predict collisions to occur with a great enough frequency that there may be observational consequences. If a quark antinugget does collide with the matter comprising the visible component of the galaxy we expect the interactions to proceed at the rapid strong scale. The question then becomes whether there will be any clear observational consequences of these interactions and if so what form the resulting spectrum will take. This question is complicated by the wide range of energy scales involved from the quark chemical potential with $\mu_q \sim 500MeV$ to the lepton chemical potential of $\mu \sim 10MeV$ right down to the temperature at the eV scale. The dominant contribution to the spectrum is expected to be due to annihilation events involving antinuggets. Based on galactic abundances the majority of annihilation events are likely to involve a galactic electron or proton. Annihilation of other forms of galactic matter will also occur but with a lower frequency. Events involving larger objects are also less likely to produce a coherent detectable signal. In order to make predictions about the nature of the spectrum we will thus consider the the result of interactions between a galactic electron or proton and a quark antinugget.

3.1 Electron annihilation

A galactic electron incident on the electrosphere of an antiquark nugget will proceed through the fermi gas of positrons at a roughly constant velocity

3.1. Electron annihilation

(at the galactic scale of a few hundred kilometers per second) experiencing a rapid increase in both the positron density and the average positron kinetic energy. There are two distinct processes one should consider in treating annihilation events involving a galactic electron. If the centre of mass momentum is small then the electron positron pair will form an intermediate bound state (positronium) which will subsequently decay in a well known way producing either a pair of back to back 511keV photons or a three photon continuum. The form of this spectrum has been measured in scattering experiments and is well known. This process is a resonance effect and thus it proceeds at a relatively fast rate which will remain essentially constant over the regions of the electrosphere at which the densities are not vanishingly small. As one moves off resonance, that is to higher momenta, the probability of forming positronium falls rapidly and direct QED annihilation events begin to dominate. For these events the growth of the density of states with positron momentum favors annihilations involving positrons near the fermi surface. In this case the form of the spectrum may be determined from a relatively straight forward QED calculation the details of which will be worked through below. The end result is that the annihilation of galactic electrons will produce a positronium decay line at 511keV as well as a broad continuum at the MeV scale with maximum energies near the lepton chemical potential at the quark matter surface. The relative strength of these two emission mechanisms may be found from the relative rates at which the two processes proceed. While the exact probability of positronium formation is a complicated quantum mechanical problem involving a summation over all positronium states, however a reasonable approximation may be obtained by considering the overlap of the incident e^+e^- wavefunctions with the ground state wavefunction of positronium (for details see appendix B.) From these considerations one predicts a formation rate for positronium of $\tau_{Ps}^{-1} \sim v_e m \alpha$ where v_e is the incident electron velocity which should be at a typical galactic scale of a few hundred kilometers per second. Performing a similar calculation for the annihilation of a galactic electron within the electrosphere of an antiquark nugget is an exercise in QED. This calculation involves computing the rate at which $e^+e^- \rightarrow photons$ as a function of the local chemical potential and the final state photon energy. It is performed in detail in appendix C. The essential point of these calculations is that, if the dark matter is composed of colour superconducting nuggets as argued here, it will necessarily produce a positronium decay line along with it's associated continuum as well as a broad MeV emission spectrum with a total energy flux below that of the positronium spectrum. The shape of the MeV spectrum will rise quickly to a peak near 511keV and then fall with increas-

ing energy. It should be stressed that these two distinct spectral features are required by the dark matter model under consideration and are based entirely in well known physics with no free parameters. If spectral features matching these results were not to be found in the diffuse emissions from the galactic centre then the model would be invalidated.

3.2 Comparison with observation

3.2.1 The galactic 511keV line

Observations of the galactic centre do in fact detect a 511keV positron annihilation line. SPI/INTEGRAL data shows evidence for both a core and fainter disk component. The spectrum from the core is found to be roughly gaussian with an average flux of $\frac{d\Phi}{d\Omega} \simeq 0.025$ photons $cm^{-2}s^{-1}sr^{-1}$ [5, 7]. This emission feature implies a large number of low momentum positrons are present in the galactic centre however no astrophysical phenomenon has been proposed to produce them in sufficient quantities. For the purposes of what follows it will be assumed that the vast majority of the 511keV line has as its source the annihilation of galactic electrons in the electrosphere of an antinugget.

3.2.2 Diffuse MeV emissions from the galactic core

The case of the MeV continuum is more complex than that of the 511keV line. Without a distinct spectral feature to search for one is forced to perform a complicated background subtraction across a relatively large energy range. In the relevant regime there are relatively few contributing point sources, instead the majority of the diffuse background may be attributed to the scattering of cosmic rays off the galactic medium. Fortunately the spectrum attributed to cosmic ray processes has been studied for purposes apart from those discussed here [11]. While current models produce accurate energy and spacial distributions across a wide range in energy there is a distinct excess of emissions detected in the MeV energy range where the COMPTEL satellite has made several observations. This excess seems to be strongly correlated with the galactic centre. Details of this spectrum along with the cosmic ray spectrum are depicted in figure 3.2.2. While the preceding section gave a relative scale for the 511keV line and the MeV continuum no absolute energy scale was given. The difficulty in arriving at an absolute magnitude for the emission mechanisms discussed is due to uncertainties in the number density of both visible and dark matter in the galactic core.

3.2. Comparison with observation

Even if the mass density was precisely known there would remain a large uncertainty in the number density of the nuggets due to their wide range in possible baryon number. To circumvent this difficulty the strength of the 511keV line from the galactic center will be used as normalization from which the scale of the MeV emission may be determined. Comparison of the predicted MeV spectrum with observations of the galactic centre will then provide a nontrivial test of the quark nugget dark matter model. The complete annihilation spectrum integrated over all depths was obtained in appendix C C.7. However the overall scale was at that point arbitrary as the entire spectrum was scaled by an undetermined constant n_∞ . To predict the resulting MeV spectrum from the galactic centre we will use the strength of the 511keV line as normalization. The total strength of the positronium decay line is also dependent on n_∞ . Similar to the calculations for the direct annihilation spectrum the total number of positronium events may be written as,

$$N_{tot}^{Ps} = \int \frac{dz}{v_e} \frac{dn_{Ps}}{dz} = \int dz n_e(z) \frac{\Gamma_{Ps}}{v_e}. \quad (3.1)$$

Where n_e is the surviving number of galactic electrons as a function of depth within the electrosphere as evaluated in C.6 and the rate of positronium formation is $\Gamma_{Ps} = v_e m \alpha$ as discussed in appendix B. The strength of the galactic 511keV line is then,

$$N_{tot}^{Ps} = n_\infty m \alpha \int dz e^{-\Gamma/v_e} \quad (3.2)$$

The value of n_∞ will then be chosen so that the total measured flux matches the SPI/INTEGRAL data. Numerically this gives a result of $n_\infty \sim \text{NUMBER}$. This result may then be used to evaluate the final spectrum C.7. As noted in appendix C once the surface chemical potential $\mu_0 \gtrsim 20 \text{MeV}$ only a very small fraction of incident electrons will survive to the inner region of the electrosphere and thus the spectrum is almost independent of the surface conditions. A plot of this spectrum is given in figure 3.2.2 for reference the COMPTEL data points have been overlaid, a second curve is plotted in which the established cosmic ray background shown in 3.2.2 has been added to the calculated nugget spectrum. Note that both the shape of the spectrum as well as the magnitude are a good match to the COMPTEL data.

3.2.3 Other emission mechanisms

While it is not the focus of this work nearly identical considerations to those made above about the annihilation of galactic electrons can be made about

3.2. Comparison with observation

galactic protons. The brief discussion presented here is based on the detailed calculations presented in [3] [4]. A proton incident on an antiquark nugget will pass through the electrosphere and strike the colour superconducting core. The CS, being a complicated many body quantum state with a very sharp edge, has a large probability of Andreev reflecting the incident proton rather than annihilating it. Those protons which do annihilate directly will release $\sim 2\text{GeV}$ of energy in a pair of back to back jets with one jet directed towards the surface while the other thermalizes deep within the nugget. As the outward moving jet reaches the surface it will transfer most of its energy to the positrons which are the lightest available degrees of freedom. These ejected positrons with relativistic energies then pass through the strong electric fields at the quark matter surface. It can be shown that the result of this process is a burst of bremsstrahlung radiation from with a characteristic energy of roughly 10keV . As mentioned, the second jet will expend its energy deep inside the nugget. This effect proves to be the dominant factor in determining the average temperature of the nuggets. The temperature scale is set by the energy balance between proton annihilation and thermal emission from the nuggets. This thermal emission will occur from an effective surface in the electrosphere near the Boltzmann regime where the thermal photons, with energy $E \sim T \sim eV$, are first able to escape the nugget without scattering. This result makes the calculation of the thermal emission mechanism quite general regardless of the exact form of colour superconductivity realized at the core. By calculating the emissivity of the Boltzmann regime of the electrosphere it is possible to determine the resulting spectrum which is found to extend well into the microwave ($\sim 10^{-4}eV$.) As in the case of electron annihilation it is found that proton annihilation will produce a definite observational signature of dark matter as colour superconducting nuggets. As with electron annihilations, observations in the relevant energy range show an excess of flux from the galactic centre beyond that predicted by standard astrophysical considerations. In particular the Chandra satellite has detected what has been described as a plasma with a temperature of roughly 8keV closely associated with the galactic centre [9]. However, such a plasma would not remain bound to the galactic core and no possible heating mechanism is known. Within our model this “plasma” is actually the combined effect of the numerous proton annihilations occurring in the galactic centre. One consequence of this model is that, as it is based entirely on events within the nugget, the form of the resulting spectrum should be independent of the surrounding galactic environment. In the microwave range it has been suggested that the WMAP data would be better fit if the galactic spectrum includes a diffuse emission source distributed in

3.2. Comparison with observation

a roughly gaussian way around the galactic centre. Exactly this type of diffuse emissions are required by the dark matter model presented here. As in the case of the MeV emissions one can extract the matter/dark matter interaction rates from the SPI/INTEGRAL 511keV line strength and use it predict the energy scale at which the proton annihilation spectra should fall. In both the 10keV and microwave cases the total energy scales are found to be in good agreement with the Chandra and WMAP data.

3.2. Comparison with observation

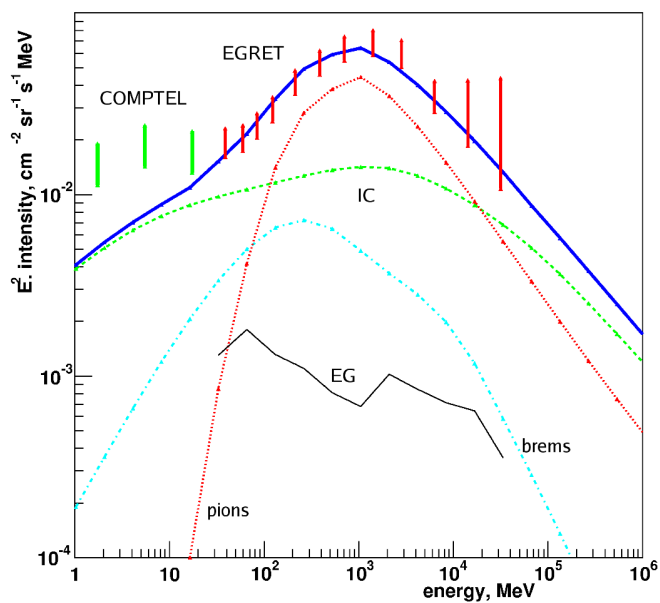


Figure 3.1: Best fit to the high energy diffuse spectrum of the galactic centre from Moskalenko et al. based on cosmic ray effects with point sources subtracted. Note the observed excess over the calculated spectrum in the COMPTEL range.

3.2. Comparison with observation

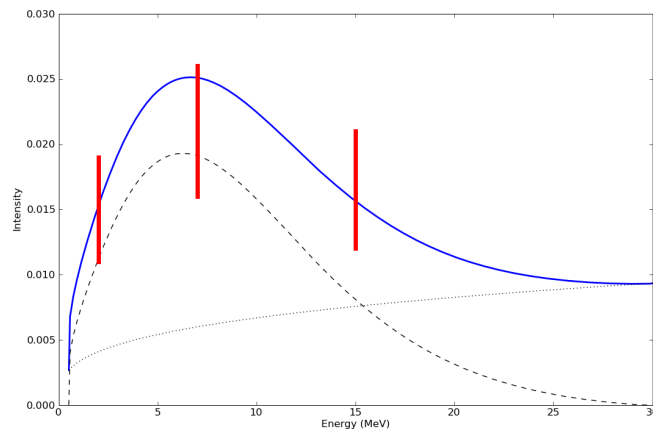


Figure 3.2: Total intensity (flattened by k^2 as in 3.2.2) averaged over all electrosphere heights. The total emission spectrum is shown in solid blue while the cosmic ray background and dark matter spectrum are shown in black dotted and dashed lines respectively. The red bars are the COMPTEL data points.

Chapter 4

Conclusion

This work is intended to convince the reader that the dark matter in the universe may in fact be ordinary matter and antimatter condensed into a non-baryonic phase and that such a model presents no contradictions with present observations. The interactions between the quark nuggets of this model and the ordinary visible matter of the galaxy may help to explain components of the galactic spectrum over a broad range on energies. It should be noted just how broad this range is, from the diffuse MeV emission continuum, to the positron annihilation line and diffuse x-ray spectrum down to the microwave contribution the emission mechanisms discussed here span some thirteen orders of magnitude. In each case the total energy budget and the form of the resulting spectrum are consistent with observation. It should also be noted that this is achieved entirely within the context of well known QED and QCD physics. In principle all quantities discussed here may be directly calculated from first principle arguments. Only the uncertainty in the dark matter distribution of the galactic core requires the use 511keV line for normalization. As this model requires no new physics and contains no tunable parameters it is much more tightly constrained than the majority of dark matter candidates. This offers the prospect of several strong tests of the model using data either presently available or which is likely to be available in the near future. In particular there should exist a strong spacial correlation between all the spectral features discussed here. This correlation must also mirror the product of the matter and dark matter densities. Also, the proton annihilation spectrum must be independent of the region of the galaxy from which it is observed. Future modeling of galactic astrophysics is also likely to tighten the constraints on this model as the relevant background contributions to the observed spectra become better understood.

As has been demonstrated here it is possible to explain both the nature of dark matter and the mechanism of baryogenesis without appealing to new physics for which we have no evidence and upon which we can place very few constraints.

Bibliography

- [1] Charles Alcock, Edward Farhi, and Angela Olinto. Strange stars. *Astrophys. J.*, 310:261–272, 1986.
- [2] Mark G. Alford, Andreas Schmitt, Krishna Rajagopal, and Thomas Schafer. Color superconductivity in dense quark matter. 2007.
- [3] Michael McNeil Forbes and Ariel R. Zhitnitsky. Diffuse x-rays: Directly observing dark matter? *JCAP*, 0801:023, 2008.
- [4] Michael McNeil Forbes and Ariel R. Zhitnitsky. WMAP Haze: Directly Observing Dark Matter? *Phys. Rev., D*, to appear, 2008.
- [5] Pierre Jean et al. Early SPI/INTEGRAL measurements of galactic 511 keV line emission from positron annihilation. *Astron. Astrophys.*, 407:L55, 2003.
- [6] D. Kharzeev and A. Zhitnitsky. Charge separation induced by P-odd bubbles in QCD matter. *Nucl. Phys.*, A797:67–79, 2007.
- [7] Jurgen Knodlseder et al. Early SPI/INTEGRAL constraints on the morphology of the 511 keV line emission in the 4th galactic quadrant. *Astron. Astrophys.*, 411:L457–L460, 2003.
- [8] Kyle Lawson and Ariel R. Zhitnitsky. Diffuse cosmic gamma-rays at 1-20 MeV: A trace of the dark matter? *JCAP*, 0801:022, 2008.
- [9] Michael P. Muno et al. Diffuse X-ray Emission in a Deep Chandra Image of the Galactic Center. *Astrophys. J.*, 613:326–342, 2004.
- [10] David H. Oaknin and Ariel Zhitnitsky. Baryon asymmetry, dark matter and quantum chromodynamics. *Phys. Rev., D*71:023519, 2005.
- [11] Andrew W. Strong, Igor V. Moskalenko, and Olaf Reimer. Diffuse Galactic continuum gamma rays. A model compatible with EGRET data and cosmic-ray measurements. *Astrophys. J.*, 613:962–976, 2004.

Chapter 4. Bibliography

- [12] V. V. Usov, Tiberiu Harko, and K. S. Cheng. Structure of the electrospheres of bare strange stars. *Astrophys. J.*, 620:915–921, 2005.
- [13] Ariel Zhitnitsky. The Width of the 511 KeV Line from the Bulge of the Galaxy. *Phys. Rev.*, D76:103518, 2007.
- [14] Ariel R. Zhitnitsky. ‘Nonbaryonic’ dark matter as baryonic color superconductor. *JCAP*, 0310:010, 2003.

Appendix A

Lepton Distributions

The distribution of leptons in the electrosphere surrounding a CS nugget may be determined based on the surface charge alone. However this is a very complex many body problem (equivalent to calculating the electron structure of an atom with $Z \gtrsim 10^{20}$.) As a primary step to be used throughout what follows the electrosphere will be modeled as a fermi gas for which the density is given by,

$$n = \int_0^\infty \frac{2d^3\vec{p}}{(2\pi)^3} \frac{1}{1 + e^{(E-\mu)/T}}. \quad (\text{A.1})$$

This approximation treats the leptons of the electrosphere as non-interacting and should be quite good in the highly degenerate regime near the quark surface where all interactions are gapped. Obviously this will break down in the long distance tail of the electrosphere where degeneracy effects become progressively less important. However the densities in this regime are sufficiently small that they have little impact on the final interaction calculations.

The simplest result is obtained by taking the temperature to be much smaller than any other scales in the problem at which point the fermi function behaves as a step function and the electrosphere is governed by the expression 2.2. First we consider the plane parallel case. Here the second order differential equation may be reduced to first order as,

$$\begin{aligned} \left(\frac{d\mu}{dz}\right)^2 &= \frac{8\alpha}{3\pi} \int d\mu (\mu^2 - m^2)^{3/2}, \\ \frac{d\mu}{dz} &= \left(\frac{3\pi}{8\alpha}\right)^{3/2} \left[\frac{\mu}{4} (\mu^2 - m^2) - \frac{3}{8} \mu m^2 (\mu^2 - m^2)^{1/2} \right. \\ &\quad \left. + \frac{3}{8} m^4 \ln \left(\frac{\mu + (\mu^2 - m^2)^{1/2}}{\mu - (\mu^2 - m^2)^{1/2}} \right) \right]. \end{aligned} \quad (\text{A.2})$$

This differential equation does not have a simple closed form however it is quite simple to evaluate numerically. This may be done by converting the differential equation to an integral equation and performing a numerical

Appendix A. Lepton Distributions

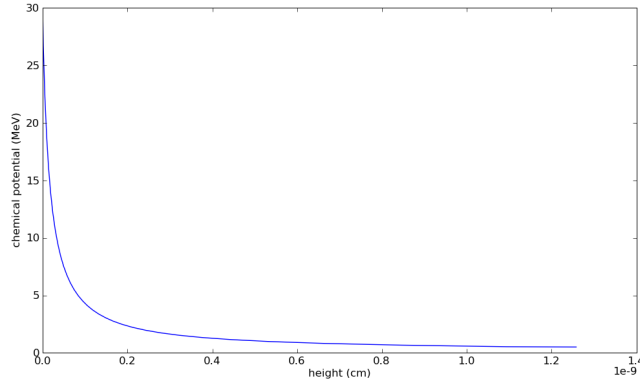


Figure A.1: Chemical potential as a function of height. Here the surface chemical potential is taken to be $\mu_0 = 30MeV$.

integration starting from the quark surface taking the chemical potential at this point as a boundary condition. The result of this integration is depicted in figure A. Once the chemical potential at all radial distances is known the density may be established using the $T = 0$ expression for the density of a fermi gas, $n = \frac{(\mu^2 - m^2)^{3/2}}{3\pi^2}$. A plot of positron density is given in figure A

Appendix A. Lepton Distributions

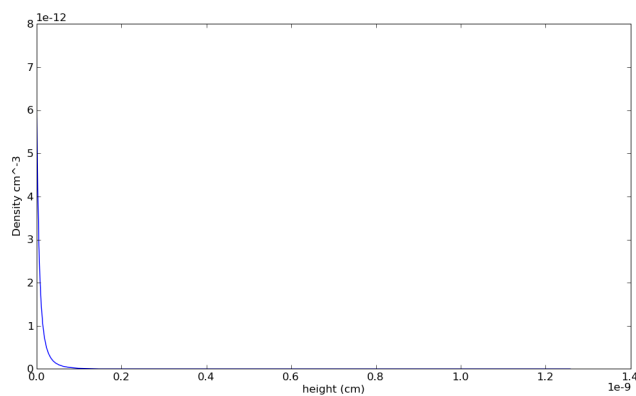


Figure A.2: Lepton density as a function of height. Here the surface chemical potential is taken to be $\mu_0 = 30MeV$.

Appendix B

Positronium Formation Rates

A complete calculation of the rate at which positronium forms from low momentum electron positron collisions is beyond the scope of this work. Such a calculation would entail calculating the overlap of the incident particle wavefunctions with all states of positronium and a summing over all resulting terms. Instead, following [13], consider the overlap between a low momentum electron positron pair represented by incoming plane waves with the positronium ground state only. First we note that the ground state of positronium is $|\psi_{1,0,0}\rangle = \frac{1}{(\pi a^3)^{1/2}} e^{-r/a}$, where $a = (m\alpha)^{-1} \approx 10^{-8} \text{cm}$ is the Bohr radius. The overlap of this wave function with the center of mass plane waves corresponding to the e^+e^- pair is,

$$\langle \psi_{1,0,0} | \psi_{e^+e^-}(q) \rangle \sim \int d^3r e^{-r/a} e^{irq} \sim \frac{1}{1 + a^2 q^2} \quad (\text{B.1})$$

Where q is the centre of mass momentum and the overall constant, which is not relevant to our purposes, has been neglected. The main result of this calculation is that the probability of forming positronium (which is of course $|\langle \psi_{1,0,0} | \psi_{e^+e^-}(q) \rangle|^2$) falls rapidly when the centre of mass momentum becomes larger than $m\alpha$, when the momentum is smaller than this the probability of order one. For simplicity the branching fraction to positronium will be taken as

$$\frac{n(e^+e^- \rightarrow Ps)}{n(\text{total})} = \begin{cases} 1 & \text{if } \mu < m\alpha \\ 0 & \text{if } \mu > m\alpha \end{cases} \quad (\text{B.2})$$

The exponential behavior of the positronium wave function also introduces the Bohr radius as a natural length scale. If the colliding electron and positron are within one Bohr radius then the probability of positronium formation is high, consequently the cross section for positronium formation should be $\sigma_{Ps} \sim 4\pi(m\alpha)^{-2}$. Under these assumptions the total rate at

Appendix B. Positronium Formation Rates

which positronium is formed will be,

$$\Gamma_{Ps} = \int dn(p)v\sigma \sim nv_e\pi(m\alpha)^{-2} \sim v_e\pi m\alpha \quad (\text{B.3})$$

Where we have taken the relative velocity to be at the typical galactic velocity of $v_e \sim 0.001$ and have noted that the density corresponding to a fermi momentum of $p_F \sim m\alpha$ is simply $n \sim (m\alpha)^3$ up to geometric factors. It is this value of the positronium formation rate that will be used in subsequent calculations.

Appendix C

The direct annihilation spectrum

This appendix details the process by which the spectrum arising from galactic electrons annihilating in the electrosphere of an antiquark nugget may be obtained. An essentially identical calculation was performed in [8]. Those galactic electrons which do not annihilate through the positronium channel will instead annihilate through a direct $e^+e^- \rightarrow \text{photons}$ QED process. The differential cross section for this process is well known (it seems to have been first calculated by Dirac) and is found to be,

$$\begin{aligned} \frac{d\sigma}{dk} &= \frac{\pi\alpha^2}{mp^2} \left[\frac{-(3m+E)(m+E)}{(m+E-k)^2} - 2 \right] \\ &+ \frac{\pi\alpha^2}{mp^2} \left[\frac{\frac{1}{k}(3m+E)(m+E)^2 - (\frac{m}{k})^2(m+E)^2}{(m+E-k)^2} \right] \end{aligned} \quad (\text{C.1})$$

Here E is the energy of the positron, m is the electron mass and k is the final state photon momentum. The rate at which photons of a given energy are produced for a given chemical potential then follows from a scattering calculation.

$$\frac{dN(k, \mu)}{dkdt} = \int dn(p)v(p) \frac{d\sigma(p, k)}{dk} = \int \frac{2d^3(p)}{(2\pi)^3} \frac{p}{E} \frac{d\sigma(p, k)}{dk}. \quad (\text{C.2})$$

Where $\frac{dN(k, \mu)}{dk dt}$ is the number of photons produced per energy per unit time and the $T \rightarrow 0$ limit has been taken for simplicity. The integration over positron momenta may be performed to give the exact form of the resulting spectrum.

$$\begin{aligned} \frac{dI(k, \mu)}{dkdt} &= \frac{\alpha^2}{\pi mk^2} \left[k(k^2 + 2mk - 2m^2) \ln \left(\frac{(2k-m)(\mu+m-k)}{mk} \right) \right. \\ &\quad \left. - \frac{3}{2}k^3 - (\mu+5m)k^2 + \left(\frac{1}{2}\mu^2 + 3\mu m + \frac{9}{2}m^2\right)k - m^2(\mu+m) \right. \\ &\quad \left. + \frac{k^2m^2}{\mu+m-k} + (8k^4 - 8mk^3 - \frac{5}{2}m^2k^2 + 4m^3k - m^4) \frac{k}{(2k-m)^2} \right]. \end{aligned} \quad (\text{C.3})$$

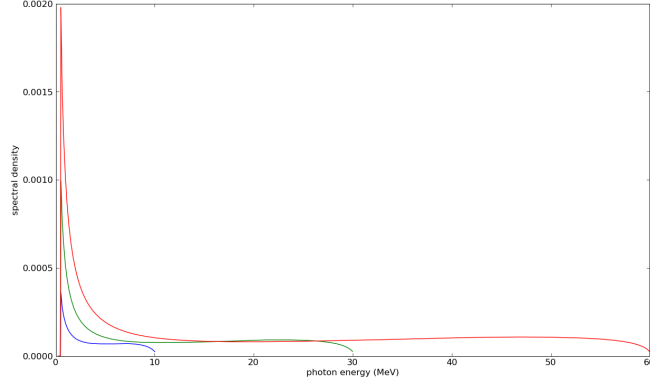


Figure C.1: Spectral density as a function of photon energy (with arbitrary normalization.) Plotted for $\mu = 10\text{MeV}$ (blue), $\mu = 30\text{MeV}$ (green) and $\mu = 60\text{MeV}$ (red.) The spectra have been rescaled by $\frac{1}{\mu}$ for to allow multiple curves on the same axes.

This function is plotted for several values of the positron chemical potential in figure C. While the function C.3 is rather complicated its general form is easily understood. The differential cross section falls off due to phase space constraints as the photon momentum is increased while the density of positrons in the fermi gas increases rapidly as you approach the fermi surface. As such the resultant spectrum spans energies from slightly below the electron mass to just above the chemical potential and is roughly flat across much of this range. The peak at the lower end of the spectrum is due to the pole at $k \rightarrow 0$.

As discussed in appendix A there are several increasingly complicated methods for modeling the positron distribution in the electrosphere of an antiquark nugget. Here it will be sufficient to consider the $T \rightarrow 0$ limit. This gives a reasonably accurate density profile over a large fraction of the radial extent of the electrosphere while remaining simple enough for demonstrative purposes. Thus the density distribution is as shown in figure A and the chemical potential as in figure A. In order to obtain the spectrum which results from a galactic electron moving through the entire electrosphere an integration over all heights weighted by the probability of reaching each height must be performed.

To begin this calculation one must calculate the rate at which galactic

Appendix C. The direct annihilation spectrum

electrons will be annihilated for a given chemical potential. As noted above positronium events occur at a constant rate through the electrosphere of $\Gamma_{Ps} \sim v_e \pi m \alpha$. The direct annihilation rate is obtained by integrating the spectral density C.3 over all outgoing photon energies $\Gamma_{dir} = \int dk \frac{dI}{dkdt}$. Then at each height the number of incident electrons will be extinguished at a rate determined by the differential equation

$$\frac{dn_e}{dt} = -n_e(z) (\Gamma_{dir}(z) + \Gamma_{Ps}) \quad (C.4)$$

$$\frac{dn_e}{dz} = -\frac{n_e(z)}{v_e} (\Gamma_{dir}(z) + \Gamma_{Ps}) \quad (C.5)$$

where n_e is the number of galactic electrons surviving to reach a given height and v_e is the average velocity of incident electrons¹. The differential equation has been transformed into the second form presented here for future convenience. The dependence of Γ_{dir} on the chemical potential (and thus height) makes this equation difficult to evaluate explicitly. The solution will take the form,

$$n_e(z) = n_\infty e^{-\int_\infty^z dz (\Gamma_{dir}(z) + \Gamma_{Ps}) / v_e} \quad (C.6)$$

where n_∞ is the number of galactic electrons incident on the nugget. In order to extract the resultant spectrum the annihilation rate as a function of chemical potential must be combined with the spectrum produced at a particular chemical potential as given in C.3. This is done by an integration over all heights weighted by the annihilation rate at each height.

$$\begin{aligned} \frac{dI_{tot}}{dkdt} &= \int dz \frac{dn_{dir}(z)}{dz} \frac{dI(z)}{dkdt} \\ \frac{dI_{tot}}{dkdt} &= \int dz n_e \Gamma_{dir} \frac{dI(z)}{dkdt} \\ \frac{dI_{tot}}{dkdt} &= n_\infty \int dz e^{-\int dz \Gamma_{tot} / v_e} \Gamma_{dir} \frac{dI(z)}{dkdt} \end{aligned} \quad (C.7)$$

While this integration is difficult due to the z dependence in the exponential factor it may be evaluated numerically. The results are depicted in figure 3.2.2 along with COMPTEL data points as discussed above.

¹There remains a large uncertainty in the distribution of electron velocities in the galactic centre as the final spectrum will be found do have an exponential factor with dependence on v_e this value will dominate the uncertainty in the calculations which follow.